Since January 2020 Elsevier has created a COVID-19 resource centre with free information in English and Mandarin on the novel coronavirus COVID-19. The COVID-19 resource centre is hosted on Elsevier Connect, the company's public news and information website.

Elsevier hereby grants permission to make all its COVID-19-related research that is available on the COVID-19 resource centre - including this research content - immediately available in PubMed Central and other publicly funded repositories, such as the WHO COVID database with rights for unrestricted research re-use and analyses in any form or by any means with acknowledgement of the original source. These permissions are granted for free by Elsevier for as long as the COVID-19 resource centre remains active.

Virus Research 146 (2009) 73–80

Contents lists available at ScienceDirect

Virus Research

journal homepage: www.elsevier.com/locate/virusres

Stem-loop structure of *Cocksfoot mottle virus* RNA is indispensable for programmed −1 ribosomal frameshifting

Tiina Tamm[a], Jaanus Suurväli[b], Jimmy Lucchesi[c,1], Allan Olspert[b], Erkki Truve[b,*]

[a] *Institute of Molecular and Cell Biology, University of Tartu, Riia 23, Tartu 51010, Estonia*
[b] *Department of Gene Technology, Tallinn University of Technology, Akadeemia tee 15, 12618 Tallinn, Estonia*
[c] *Institute of Biotechnology, P.O. Box 56, 00014 University of Helsinki, Finland*

ARTICLE INFO

Article history:
Received 13 April 2009
Received in revised form 8 August 2009
Accepted 2 September 2009
Available online 11 September 2009

Keywords:
Cocksfoot mottle virus
Sobemovirus
Ribosomal frameshift
RNA structure
RNA stem-loop
Local and systemic infection

ABSTRACT

The −1 programmed ribosomal frameshifting (−1 PRF) mechanism utilized by many viruses is dependent on a heptanucleotide slippery sequence and a downstream secondary structure element. In the current study, the RNA structure downstream from the slippery site of cocksfoot mottle sobemovirus (CfMV) was proven to be a 12 bp stem-loop with a single bulge and a tetranucleotide loop. Several deletion and insertion mutants with altered stem-loop structures were tested in wheat germ extract (WGE) for frameshifting efficiency. The impact of the same mutations on virus infectivity was tested in oat plants. Mutations shortening or destabilizing the stem region reduced significantly but did not abolish −1 PRF in WGE. The same mutations proved to be deleterious for virus infection. However, extending the loop region to seven nucleotides had no significant effect on frameshifting efficiency in WGE and did not hamper virus replication in infected leaves. This is the first report about the experimentally proven RNA secondary structure directing −1 PRF of sobemoviruses.

© 2009 Elsevier B.V. All rights reserved.

1. Introduction

Many positive strand RNA viruses use −1 programmed ribosomal frameshifting (−1 PRF) for regulating the expression of viral polymerases. Two *cis*-acting elements are required for an efficient −1 PRF. First, a seven nucleotide slippery sequence is the place where the ribosome will slip back by one nucleotide. The sequence motif for the slip-site is X XXY YYZ (preframeshift codons are indicated), where X can be any nucleotide, Y either A or U, and Z can be any nucleotide except G (Brierley et al., 1992). Secondly, the shifty heptanucleotide is followed by the sequence that is forming a downstream secondary structure. The investigated downstream stimulatory elements can be divided into three groups. The best studied group includes hairpin-type RNA pseudoknot structures formed when the nucleotides of hairpin loop base pair with single-stranded downstream complementary nucleotides (reviewed by Giedroc and Cornish, 2008). The second group of structures consists of pseudoknots having an unusual structure. For example, a three-stemmed pseudoknot structure has been reported for *Severe acute respiratory syndrome coronavirus* (Baranov et al., 2005; Brierley and Dos Ramos, 2006; Plant et al., 2005; Su et al., 2005). This structure is composed of two double-stranded stems connected by a single-stranded loop and a second loop which itself folds into a stem-loop. The stimulatory RNA of the *Visna-Maedi virus* −1 ribosomal frameshifting signal is another unusual pseudoknot with a seven nucleotide interstem element between two stems (Pennell et al., 2008). The third group includes stable stem-loop structures sufficient to promote efficient −1 PRF. Examples include the frameshift-promoting elements at the *gag-pol* junction in *Giardia lamblia virus* (GLV), *Human immunodeficiency virus* type 1 (HIV-1), *Simian immunodeficiency virus* (SIV) and related lentiviruses (Brierley and Dos Ramos, 2006; Li et al., 2001; Marcheschi et al., 2007; Staple and Butcher, 2005). The requirement for a simple hairpin loop in frameshifting has been also demonstrated in *Human astrovirus* serotype-1 (HAst-1), *Human T-cell leukemia virus* type II (HTLV-II) and *Red clover necrotic mosaic virus* RNA-1 (RCNMV) (Falk et al., 1993; Kim and Lommel, 1994, 1998; Marczinke et al., 1994).

Cocksfoot mottle virus (CfMV, unassigned genus *Sobemovirus*) is a plant virus with a monopartite, single-stranded, positive-sense RNA genome (Mäkinen et al., 1995b). The polyprotein of CfMV encodes a viral protease, VPg and an RNA-dependent RNA polymerase (RdRp). It is translated from two overlapping open reading frames, ORF 2a and 2b, by a −1 PRF mechanism (Mäkinen et al., 1995a) (Fig. 1). The consensus signals for −1 PRF were identified at the beginning of the overlap region: the slippery sequence U UUA AAC (nucleotides 1634–1640, preframeshift codons are indicated) and a predicted stem-loop structure (nucleotides 1648–1676) starting seven nucleotides

* Corresponding author. Tel.: +372 620 4422; fax: +372 620 4401.
E-mail address: erkki.truve@ttu.ee (E. Truve).
[1] Present address: Vivoxid Ltd., Biolinja 12, 20750 Turku, Finland.

0168-1702/$ – see front matter © 2009 Elsevier B.V. All rights reserved.
doi:10.1016/j.virusres.2009.09.002

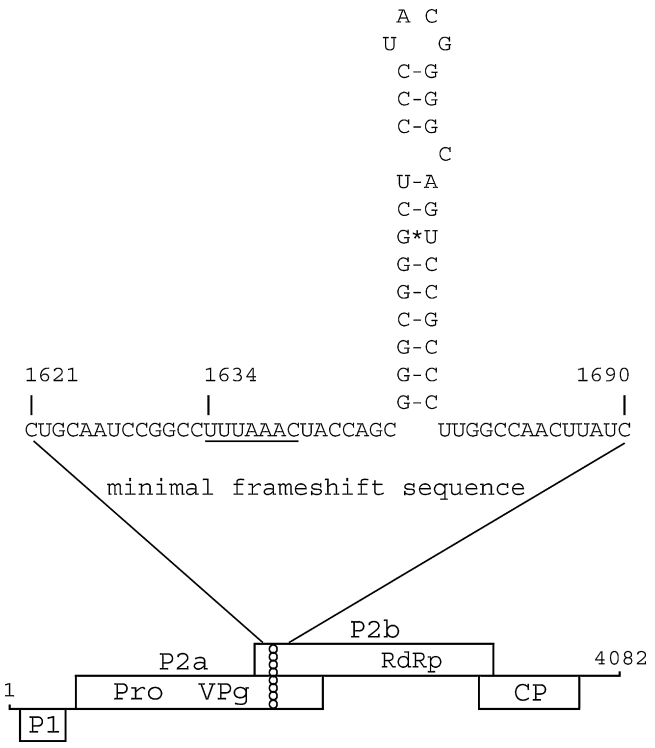

Fig. 1. Genomic organization of CfMV and *cis*-acting RNA elements involved in −1 ribosomal frameshifting. The coding regions of CfMV genome are shown by boxes. The serine protease (Pro), VPg and RNA-dependent RNA polymerase (RdRp) domains in the polyprotein are indicated. P1, ORF 1 encoded protein; P2a and P2b, ORF 2a and 2b encoded proteins; CP, coat protein. The chain label marks the position of the 70-nt minimal frameshift region required for efficient *in vitro* frameshifting. The sequence of the minimal frameshift region containing the *cis*-acting RNA elements is shown. The 7-nt slippery sequence is underlined. The downstream stem-loop secondary structure is predicted by MFOLD.

downstream. Both mutating the heptanucleotide sequence and deleting the putative secondary structure were shown to completely abolish the frameshifting activity, indicating that these *cis*-acting elements are absolutely required for −1 PRF to proceed (Lucchesi et al., 2000). The minimal frameshift sequence required for efficient *in vitro* frameshifting was mapped at the nucleotides 1621–1690 (Lucchesi et al., 2000) (Fig. 1). This 70 nucleotide sequence, containing both the slippery sequence and the predicted downstream secondary structure, was shown to direct −1 PRF in wheat germ extract (WGE) with an efficiency of 12.7 ± 1.4%. Similar *in vitro* frameshifting efficiency, 10.6 ± 1.4%, was determined for the entire ORF2a–2b encoding region (Lucchesi et al., 2000; Tamm et al., 1999).

In this study, we report that the −1 PRF signal of CfMV indeed includes a stem-loop structure as a downstream element. We have mapped the structure of the frameshifting site of CfMV by chemical probing. Several mutations were introduced to study the importance of particular structural elements in determining the frameshifting efficiency. The impact of these mutations was quantitatively analyzed by measuring the frameshifting efficiencies in a WGE *in vitro* translation system. The effects of mutating the frameshifting region on the local and systemic infection of CfMV was examined in oat plants.

2. Materials and methods

2.1. Plasmid construction

The base numbering used in this study refers to the genome of the CfMV Norwegian isolate as in Mäkinen et al. (1995b). The construction of pAB-21, containing CfMV polyprotein region (nucleotides 418–3265), has been described earlier (Lucchesi et al., 2000). This plasmid was used as a template to create all the other constructs for *in vitro* studies.

For the construction of pRF2, a fragment containing the slippery sequence and the stem-loop region (nucleotides 1604–1898) was amplified by PCR and cloned into pGEM-T Easy (Promega) under the control of T7 RNA polymerase promoter. This plasmid was used for the *in vitro* transcription experiments.

The following mutations in pAB-21 were introduced by PCR-based mutagenesis (Fig. 3A). pAB(ΔCUU) contains a deletion of a conserved CUU triplet (nucleotides 1685–1687). In the case of pAB(ΔC), the C nucleotide at position 1667 was deleted and a restriction site for ApaI introduced (nucleotides 1679–1684) to retain the reading frame. In pAB(+G), an additional G nucleotide was inserted at position 1657 and nucleotides 1683–1799 were deleted in order to restore the reading frame. Plasmids pAB(ΔCUU), pAB(ΔC) and pAB(+G) were obtained using Excite site-directed mutagenesis kit (Stratagene) according to the manufacturer's instructions. pAB(+UUU) was generated by inserting UUU at position 1662–1664. In pAB(G → U), the G nucleotide at position 1649 was mutated to U. In pAB(C → A), the C nucleotide at position 1675 was mutated to A. In pAB(G → U, C → A), the G at position 1649 and C at position 1675 were changed to U and A, respectively. These mutations were introduced as described by Meier et al. (2006). The PCR fragments carrying the mutations were cut with KpnI and Cfr42I and inserted into pAB-21 cut with the same enzymes.

The construction of the infectious cDNA of CfMV (CfMV icDNA) and replicase-deficient CfMV cDNA clone (CfMV RdRp(−)) have been described earlier (Meier et al., 2006). Three CfMV cDNA clones were constructed carrying the following mutations: in CfMV mRF(C → A), the C nucleotide at position 1675 was mutated to A; in CfMV mRF(+UUU), the UUU were inserted at position 1662–1664; in CfMV mRF(ΔC,+C), the C nucleotide at position 1667 was deleted and one extra C nucleotide inserted at position 1677 (Fig. 4A). The mutations were introduced by PCR-based mutagenesis (Meier et al., 2006). The obtained PCR fragments were cut with Cfr42I and Eco147I and inserted into an icDNA construct cut with the same enzymes.

All mutations were verified by sequencing.

2.2. RNA in vitro transcription, chemical probing and primer extension analysis

pRF2 was linearized with SalI for run-off transcription with bacteriophage T7 RNA polymerase. *In vitro* transcribed RNA was purified on a Sephadex S400 (GE Healthcare) spin column as described (Liiv et al., 1998). Modification reactions with dimethyl sulfate (DMS), 1-cyclohexyl-3-(2-morpholinoethyl)-carbodiimide metho-*p*-toluene sulfonate (CMCT) or kethoxal were done in a 50 μl reaction volume containing 20 pmol of RNA according to Liiv and Remme (2004). The unpaired bases are accessible to alkylation by these agents. DMS modifies the N3 position of cytosine and the N1 position of adenine. CMCT modifies the N3 group of uracil and N1 of guanine. Kethoxal modifies guanine residues at positions N1 and N2. Modification sites were determined by primer extension using reverse primer 117,864 (complementary nucleotides 1777–1757) and reverse transcriptase. Primer extension with [α-^{32}P]dCTP labelling was done as described earlier (Maiväli et al., 2002; Stern et al., 1988). Control experiments with untreated RNA were carried out to detect natural pauses of reverse transcription. Primer extension products were separated by 7% urea–polyacrylamide gel electrophoresis (PAGE).

2.3. Coupled wheat germ extract (WGE) translation

In vitro translation was carried out using TNT T7 Coupled Wheat Germ Extract System (Promega) in the presence of [^{35}S]methionine. The plasmids were linearized with NdeI before adding to the reaction mixture. Translation products were separated by 10% SDS–PAGE and detected on dried gels using Bio-Rad Molecular Imager System GS-525. The images were analyzed using Molecular Analyst Software (Bio-Rad). The relative amount of frameshifted product versus P2a was calculated from five independent translations by quantifying the radioactive signal in specific areas and correcting for background and different methionine content of products.

2.4. Virus inoculation and infection analysis

CfMV icDNA and mutated cDNA constructs were linearized with SalI and used as templates for 5′ capped RNA synthesis. *In vitro* transcription was carried out as described earlier (Meier et al., 2006). Gold particles (diameter 0.3-3.0 μm, ChemPur) were coated with transcribed RNA. Two-weeks old oat plants (cv. Jaak) were infected biolistically using Helios Gene Gun (Bio-Rad). In one experimen-

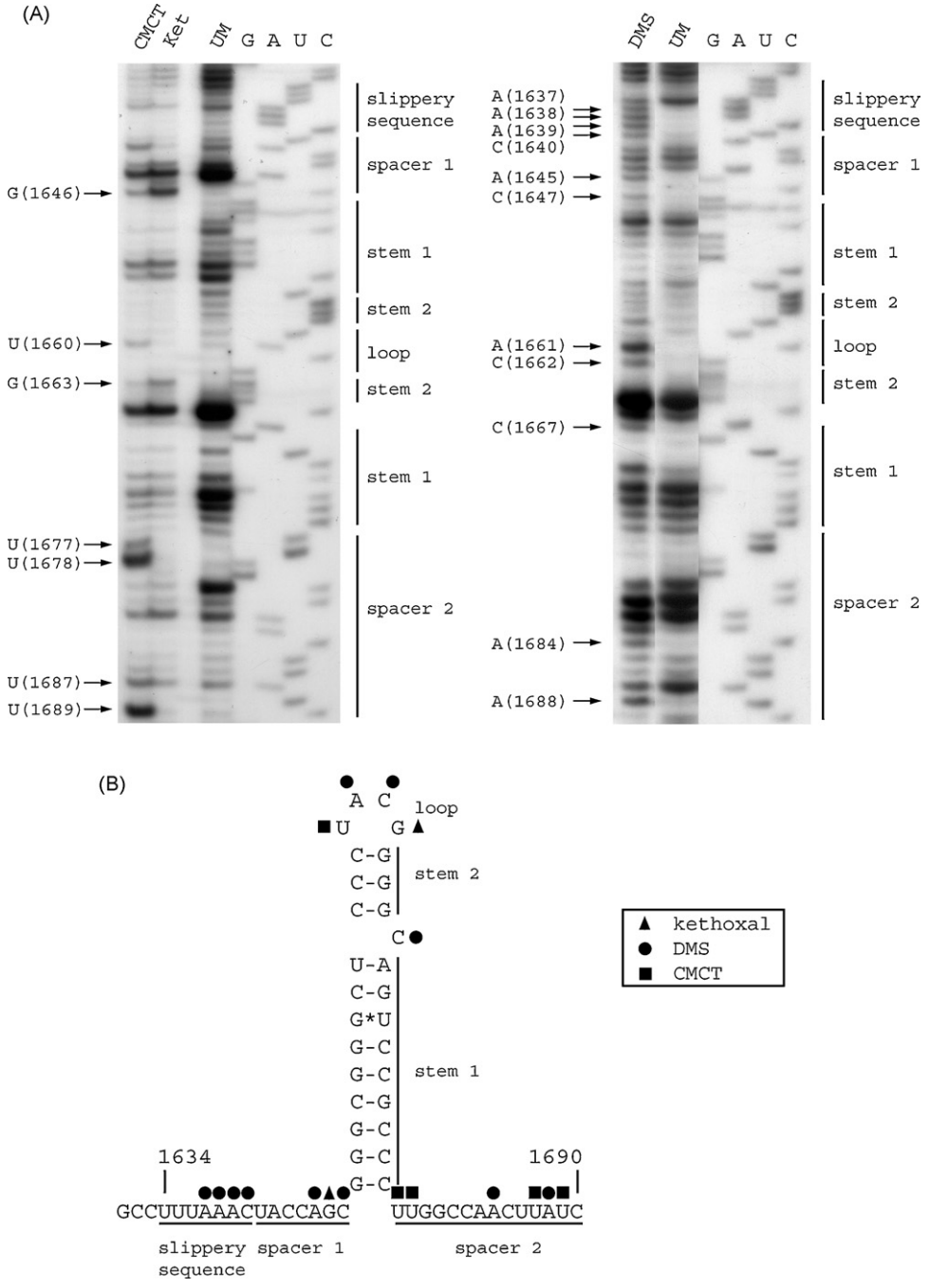

Fig. 2. Chemical probing of the RNA structure at CfMV minimal frameshift site. (A) A pRF2-derived transcript was modified by 1-cyclohexyl-3-(2-morpholinoethyl)-carbodiimide metho-*p*-toluene sulfonate (CMCT), kethoxal (Ket) or dimethyl sulfate (DMS), and sites of modification were mapped by primer extension. Unmodified RNA (UM) was used as a control. Lanes G, A, U, C represent the corresponding sequencing ladder of pRF2. Arrows on the left side of the panels indicate transcriptional stops from primer extension representing the chemically modified bases in the treated RNA molecule. The positions of the slippery sequence and secondary structure elements are indicated on the right side of the panels. (B) Summary of the analysis of primer extension results. The bases accessible to CMCT, kethoxal and DMS are shown by filled square, triangle and circle, respectively.

tal series, 16 oat plants were infected with one construct and the experiments were repeated at least twice.

Total RNA was extracted from infected leaves (10 dpi) and upper leaves (27 dpi) as described earlier (Meier et al., 2006). For Northern blot analysis, total RNA was separated on 1% agarose/formaldehyde gel and transferred to Hybond N+ membrane (GE Healthcare). Viral RNA was detected by hybridization with [α-^{32}P]dCTP-labelled probe specific for the CfMV coat protein region (nucleotides 3093–3857). The signal was detected with Personal Molecular Imager FX (Bio-Rad).

RT-PCR with primers detecting the positive strand of viral RNA was performed according to Meier et al. (2006). To verify the presence of the mutation in viral RNA, the region containing the mutation site was amplified from total RNA isolated from infected or upper leaves by RT-PCR. The obtained RT-PCR products were purified from the gel and the region containing the signals for −1 PRF was sequenced.

3. Results

3.1. A stem-loop structure constitutes the structural element for CfMV −1 ribosomal frameshifting

Computer-based analysis of CfMV ORF2a–2b overlapping region (nucleotides 1604–1710) predicted a stem-loop structure seven nucleotides downstream from the slippery sequence (Mäkinen et al., 1995a). To experimentally define the structure, the conformation of the CfMV RNA in the frameshift region was investigated using chemical modification approach. Results from chemical probing and primer extension experiments of the *in vitro* transcript of pRF2 are shown in Fig. 2A. These results are summarized on the secondary structure model in Fig. 2B.

Chemical probing experiments showed that the spacer region 1 between the slippery sequence and the stem structure (nucleotides 1641–1647) is single-stranded. Positions A (1645) and C (1647) were accessible to DMS, and G (1646) to kethoxal, respectively. Stems 1 and 2 were protected from chemical modifications as expected for base-paired stem regions. Also the G (1654)–U (1670) pair in stem 1 was inaccessible, indicating the formation of an intrahelical wobble pair. The proposed tetraloop (loop, nucleotides 1660–1663) in the end of stem 2 was completely exposed, as was a bulged C at position 1667. In the loop, U (1660) was modified by CMCT, A (1661) and C (1662) by DMS, and G (1663) by kethoxal, respectively. The bulged C (1667) was hit by DMS. The accessibility of the tetraloop rules out the potential involvement of 5′-UACG-3′ nucleotides in forming a pseudoknot. The spacer region 2 (1677–1690) appears to be single-stranded. Several positions were chemically modified beginning with a CMCT modification of U (1677).

3.2. Mutations that shorten or destabilize the stem in the stem-loop structure decrease the efficiency of −1 ribosomal frameshifting

To further evaluate the role of various secondary structure elements in frameshifting, we performed extensive site-directed mutagenesis of the frameshift region (Fig. 3A). The CfMV polyprotein encoding construct pAB-21 and individual mutants were analyzed for their ability to promote −1 frameshifting *in vitro* in WGE system (Fig. 3B). For pAB-21, the frameshifting efficiency in WGE was calculated to be 11.1 ± 1.3% (Fig. 3C), value similar to those seen in previous studies (Lucchesi et al., 2000; Tamm et al., 1999).

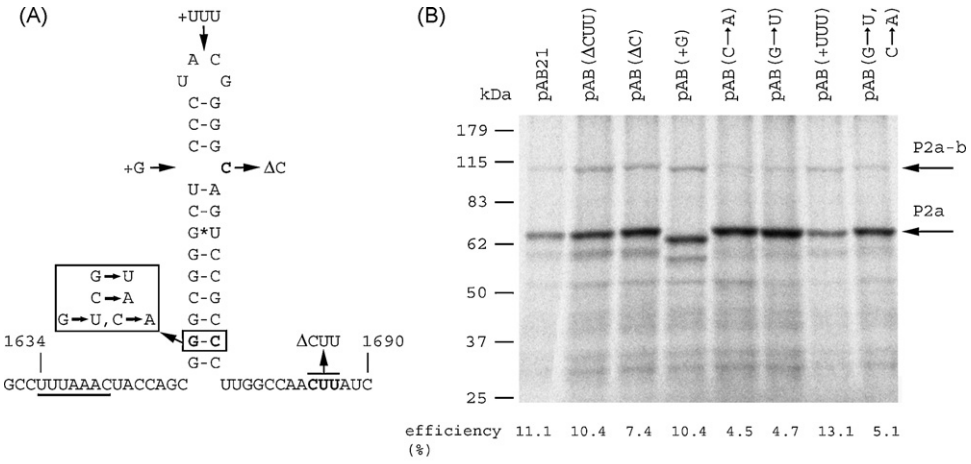

(C)

Construct	Description	Frameshift efficiency (%)
pAB-21	WT	11.1 ± 1.3
pAB(G→U)	G(1649) mutation to U	4.7 ± 0.8
pAB(C→A)	C(1675) mutation to A	4.5 ± 0.9
pAB(G→U, C→A)	G(1649) mutation to U, C(1675) mutation to A	5.1 ± 0.6
pAB(ΔC)	C(1667) deletion	7.4 ± 0.8
pAB(+G)	G insertion at 1657	10.4 ± 0.9
pAB(+UUU)	UUU insertion at 1662-1664	13.1 ± 1.5
pAB(ΔCUU)	CUU (1685-1687) deletion	10.4 ± 1.1

Fig. 3. The effect of different mutations in the CfMV minimal frameshift region on the *in vitro* frameshift efficiency. (A) The schematic representation of CfMV frameshift site. The slippery sequence is underlined, the downstream stem-loop structure and the introduced mutations are indicated. (B) Results of 10% SDS-PAGE analysis of [^{35}S]methionine-labeled translation products from the *in vitro* frameshifting assay of pAB21 construct and different mutants. The positions of the non-frameshifted P2a and frameshifted P2a–b products are indicated by arrows. The calculated frameshift efficiencies are shown in the bottom of the gel. (C) Summary of the mutations made and the resulting frameshift efficiencies in WGE. The quoted frameshift efficiencies are the average of five independent translation reactions.

Based on the structure mapping data, stem 1 of the stem-loop structure contains 6-bp G–C/C–G double-stranded stretch. To test the necessity of this paired region in frameshifting, two variants of mutants were generated (Fig. 3A). Firstly, the nucleotide on one side of the second GC-pair was mutated to disrupt the base pairing. The substitution of G (1649) with uridine or C (1675) with adenosine, both resulted in twofold reduction (from 11.1 ± 1.3% to 4.7 ± 0.8% or 4.5 ± 0.9%, respectively) of the frameshifting efficiency (Fig. 3B and C). Secondly, the second G–C base pair was replaced with the U–A base pair. The compensatory mutations (G1649 → U, C1675 → A) that should restore the base-paired structure of stem 1 did not restore wild type levels of frameshifting (efficiency 5.1 ± 0.6%; Fig. 3B and C), demonstrating the necessity of an intact G–C/C–G-base-paired segment during −1 PRF.

We also investigated whether the 5′-UACG-3′ tetraloop participates in the frameshift event. The structure mapping data already ruled out the possibility of an RNA pseudoknot formation. To assess whether the size of the loop is important, three extra U nucleotides were inserted at the position 1662–1664 (Fig. 3A). We found that this mutation did not noticeably affect the frameshifting efficiency (13.1 ± 1.5%; Fig. 3B and C).

Two constructs were generated to examine the requirement of the bulged C residue at position 1667 for an efficient −1 PRF (Fig. 3A). In mutant pAB(ΔC), the C at position 1667 was deleted, whereas in construct pAB(+G), one extra G was introduced to the position 1657 to form the G–C base pair. In both constructs, additional mutations were introduced after the minimal frameshifting region to maintain translational reading frame. Deletion of the bulged C caused a moderate but significant reduction (from 11.1 ± 1.3% to 7.4 ± 0.8%) in the −1 PRF efficiency (Fig. 3B and C). However, the insertion of one extra G did not affect the frameshifting efficiency noticeably (efficiency 10.4 ± 0.9%; Fig. 3B and C).

The analysis of putative sobemoviral frameshifting signals showed that the motif CUU, located eight nucleotides downstream from stem-loop structure, is conserved in nearly all sequenced sobemoviruses (Fig. S1). To test the relevance of this motif for −1 PRF, a construct pAB(ΔCUU) was created in which the conserved CUU (nucleotides 1685–1687) was deleted (Fig. 3A). The resulting frameshifting efficiency was similar to that of wild type (efficiency 10.4 ± 1.1%; Fig. 3B and C).

3.3. The effect of mutations in stem-loop structure on virus infectivity

To examine the role of the stem-loop structure in viral infection, we constructed three mutant CfMV cDNAs. Based on the data from *in vitro* frameshift assays, the substitution of C (1675) with adenosine in the stem 1 and deletion of bulged C (1667), both reduced frameshifting efficiency. In contrast, the insertion of three extra U nucleotides in the loop (to position 1662–1664) did not have a noticeable effect on −1 PRF. These mutations were introduced into CfMV icDNA by site-directed mutagenesis (Fig. 4A). To maintain the reading frame in CfMV mRF(ΔC,+C) construct, one extra C nucleotide was inserted to position 1667. The single amino acid changes in 0 and −1 reading frames resulted from the mutations are indicated in Fig. 4A. A replication defective CfMV cDNA clone, CfMV RdRp(−), which produces a severely truncated polyprotein, was used as a negative control.

As shown in Fig. 4B, CfMV icDNA and the mutant CfMV mRF(+UUU) were able to induce viral infection (lanes 1 and 2, and 7 and 8). Viral RNA was detected in infected leaves 10 days after bombardment and there was no difference between the wild type and the CfMV mRF(+UUU) construct. The analysis of the upper systemic leaves revealed that wild type as well as the mRF(+UUU) mutant had also the ability to spread systemically. Sequence analysis of RT-PCR fragments amplified from RNA extracted from infected and upper leaves revealed that the insertion of UUU in the loop was maintained in these viruses (data not shown). *In vitro* transcripts from CfMV RdRp(−), CfMV mRF(C → A), and CfMV mRF(ΔC,+C) mutants failed to produce any detectable signal of viral RNA in inoculated leaves (Fig. 4B, lanes 3–5), indicating that the mutations shortening the structure of stem 1 totally abolish the virus infection.

4. Discussion

We analyzed the RNA structure of the CfMV frameshift site by secondary structure probing and by site-directed mutagenesis coupled with an *in vitro* frameshifting assay and *in vivo* virus infectivity tests. The results revealed that the CfMV frameshift-promoting secondary structure element is a stem-loop starting seven nucleotides downstream from the slippery sequence. The results of the structure-probing experiments correlated with the previously predicted structure (Mäkinen et al., 1995a), as the spacer regions 1 and 2, the loop, and bulged C nucleotide were found highly accessible to alkylation by chemicals that modify single-stranded nucleotides (Fig. 2). Up to now, 11 sobemovirus genomes have been fully sequenced. All sequenced sobemoviruses exhibit common genomic organization: the RdRp is encoded by ORF2b by the −1 PRF mechanism (McGavin and Macfarlane, 2009; Meier and Truve, 2007; Sérémé et al., 2008). The analysis of their *cis*-acting −1 PRF signals indicate the presence of an identical UUUAAAC slippery sequence, a seven nucleotide spacer region 1 (exception is *Ryegrass mottle virus* where the spacer is 8 nucleotides long), and a putative stem-loop secondary structure (Fig. S1). We hypothesize that similar to CfMV, other sobemoviruses also utilize stem-loop structures rather than pseudoknots to promote frameshifting.

The comparison of sobemovirus stem-loop structures revealed that G–C composition is highly conserved in all 11 analyzed sequences (Fig. S1). The beginning of the stem 1 is G–C rich, containing in most cases at least five G–C/C–G pairs followed by an A–U pair, a G–U wobble pair or a bulged nucleotide. The disruption of the second G–C pair by mutating G (1649) to U or C (1675) to A, reduced the frameshifting efficiency *in vitro* twofold compared to the wild type structure. Replacing C (1675) with A in the full length CfMV cDNA clone abolished the virus replication in inoculated oat leaves. It is important to note that this mutation causes one amino acid change (proline to histidine) in P2a (Fig. 4A) and may affect virus infectivity. However, the C (1675) to A mutation has an effect on the secondary structure causing the stem 1 to shorten by two base pairs and extending the spacer region 1 by two nucleotides.

The cryo-electron microscopy images (∼16 Å) of a mammalian 80S ribosome-mRNA pseudoknot complex that is stalled in the process of −1 frameshifting has allowed to propose a mechanical explanation for −1 PRF (Namy et al., 2006). According to this model, the pseudoknot blocks the mRNA entrance channel and the ribosome becomes stalled during the translocation phase of the elongation cycle. The P- and A-sites of stopped ribosome must locate over the slippery heptameric sequence. Should the mutation extend the spacer region, the ribosome will pause downstream of the slippery sequence and the probability for it to slip back by 1 nucleotide is reduced. In most cases where −1 PRF is proposed or confirmed to occur, the distance between the slippery sequence and downstream RNA structure is 5–9 nucleotides (Giedroc et al., 2000). The significance of the optimal spacer length has been systematically investigated using *Infectious bronchitis virus* (IBV)-derived frameshift signal (Kontos et al., 2001; Napthine et al., 1999). The alteration of the 6-nt spacer as little as a single nucleotide either way reduced frameshifting efficiency *in vitro* indicating that the precise distance is important. The proposed −1 PRF model also indicates the importance of the strength of the downstream element.

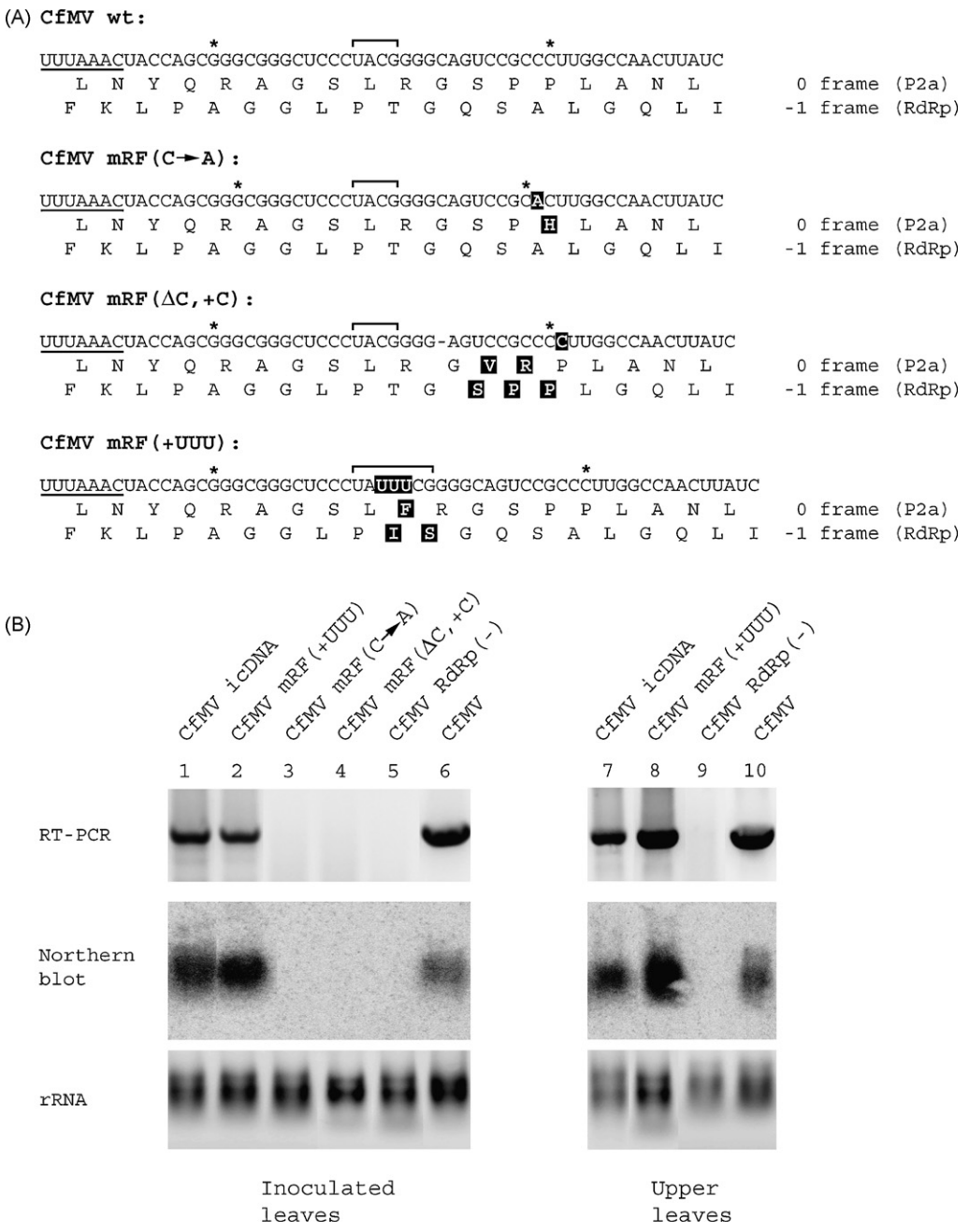

Fig. 4. The effect of different mutations in CfMV stem-loop structure on virus infectivity. (A) Summary of the mutations introduced into the CfMV cDNA to modify the stem-loop structure. The nucleotide and deduced amino acid sequences of CfMV frameshift site are shown. The slippery sequence is underlined, the beginning and end of the stem 1 is indicated by stars, the loop is shown by square bracket. P2a is translated in 0 frame, RdRp is translated in −1 frame. The introduced mutations and the resulted changes in the amino acid sequence are shown by the black background. The deleted C(1667) is shown by line. (B) Detection of CfMV in oat plants infected with CfMV infectious cDNA (CfMV icDNA, lanes 1 and 7) or CfMV mRF mutants (CfMV mRF(+UUU), lanes 2 and 8; CfMV mRF(C → A), lane 3; CfMV mRF(ΔC,+C), lane 4) by RT-PCR and Northern blotting. Plants infected with replicase-deficient CfMV RdRp(−) mutant (lanes 5 and 9) or purified virus (CfMV, lanes 6 and 10) were used as negative or positive controls, respectively. Total RNA was extracted from inoculated or upper non-inoculated leaves. Upper panels show the RT-PCR results, middle panels correspond to Northern blot analysis and lower panels represent the rRNA loading controls stained with ethidium bromide.

Based on published studies, most viral pseudoknots are G–C rich at the bottom of stem 1 (Giedroc et al., 2000). Replacing G–C pair(s) with A–U pair(s) at the beginning of stem 1 of the IBV pseudoknot reduced the frameshifting efficiency several fold (Napthine et al., 1999). As shown in Fig. 3, the stem 1 of CfMV consists of six G–C/C–G pairs. The change of the second G–C pair with U–A pair reduced the CfMV *in vitro* frameshifting efficiency twofold. These results indicate that not only the formation of the stem with a certain length, but also the strength and stability of the formed structure are important features for inducing ribosomal frameshifting.

The structure prediction analysis of the sobemoviral frameshift-promoting structures revealed that 8 out of 11 analyzed structures contain at least one bulged nucleotide after the G–C rich stem 1 region (Fig. S1). The structure of *Mouse mammary tumour virus* pseudoknot determined by NMR demonstrated that the bulged adenine is creating a hinge between the stems 1 and 2 and therefore direct coaxial stacking of the stems is not possible (Shen and Tinoco, 1995). Instead, the pseudoknot stem 1 bends towards the major groove of stem 2 resulting in relieving the strain caused by the short loop 1. The presence of similar bent conformation has been shown

for *Beet western yellow virus* (BWYV), *Potato leaf roll virus* (PLRV), *Feline immunodeficiency virus* and HIV-1 frameshift-inducing structures (Pallan et al., 2005; Staple and Butcher, 2005; Su et al., 1999; Yu et al., 2005). The mutational analysis demonstrated that the deletion of this bulged nucleotide either causes slight reduction of the frameshifting efficiency *in vitro* in the case of BWYV, or even abolishes the frameshifting phenomenon as shown for the PLRV pseudoknot structure (Kim et al., 1999; Kim et al., 2000). However, the structure of the *Simian retrovirus* type-1 (SRV-1) pseudoknot, determined by NMR, showed that in SRV-1 the stems 1 and 2 are stacked upon each other and for that reason the intercalated base at the junction is not needed for efficient frameshifting (Michiels et al., 2001). The structure mapping data for the CfMV stem-loop structure indicates that the bulged C at position 1667 is accessible to modifiers (Fig. 2). To study the importance of the potential bent conformation, C 1667 was deleted, or a single G was inserted into the opposite stem to promote the formation of G–C base pair. The *in vitro* measured frameshifting efficiencies revealed that the stem length is important, rather than the bending. The formation of a new G–C pair by inserting one extra G did not affect the frameshifting efficiency while the deletion of the bulged C only moderately reduced it (Fig. 3). However, the deletion of bulged C in the CfMV cDNA clone abolished the viral replication in the infected leaves implicating the importance of the length of the stem region. Nevertheless, we cannot rule out the possibility that the amino acid changes in P2a and RdRp introduced due to the mutagenesis may affect the *in vivo* function of these proteins.

Canonical 5′-UNCG-3′ (N = U, A, C, G) tetraloops are the most frequently found tetraloops in bacterial 16S rRNAs (Woese et al., 1990). High resolution NMR studies have shown that they have a minimum requirement of two-pair stem to form a stable RNA hairpin (Abdelkafi et al., 1997; Molinaro and Tinoco, 1995). Because of their high thermodynamic stability, it has been proposed that the UNCG family of hairpins can serve as a nucleation site for folding. The analysis of the sobemoviral frameshift structures indicates that the 5′-UNCG-3′ tetraloop sequence present in CfMV is not conserved although the small size of the loop (usually four nucleotides) is very characteristic for these stem-loop structures (Fig. S1). Based on several evidences we ruled out the formation of a pseudoknot structure by the 5′-UACG-3′ tetraloop. The results from our chemical probing experiments indicated that the loop at the end of stem 2 is completely exposed (Fig. 2). In addition, RNA structure prediction analysis with the algorithm capable of predicting pseudoknots (PknotsRG, Reeder et al., 2007) did not indicate the formation of a pseudoknot in the CfMV frameshift region, neither in those of the other sequenced sobemovirus genomes (data not shown). Finally, the construct containing the CfMV minimal frameshifting region (nucleotides 1621–1690) in the middle of the reporter gene had similar frameshifting efficiency to a construct encoding the CfMV polyprotein (Lucchesi et al., 2000). Our results also demonstrate that the loop size is not important for efficient −1 PRF. The insertion of the three extra U nucleotides into the loop did not change the frameshifting efficiency in a cell free translation system (Fig. 3) and did not abolish the local as well as systemic infection of the virus (Fig. 4B).

CfMV is the first sobemovirus for which the secondary structure of the stem-loop regulating −1 PRF has been verified experimentally. We conclude that sobemoviruses cluster together with lentiviruses and few others (examples GLV, HAst-1, HTLV-II and RCNMV) to form an unique group of viruses that require stable stem-loops for frameshifting. Marcheschi et al. (2007) hypothesized that the nature of the RNA structure of the frameshift site is dependent upon the slippery sequence to which it is coupled. They argue that for HIV-1, HIV type 2 and SIV, stable stem-loops are sufficient to promote frameshifting because the UUUUUUA slippery site is more “slippery” than other XXXYYYZ sequences. Sobemoviruses and a few others (GLV, HAst-1, HTLV-II and RCNMV) employ the diverse sequences in slippery sites together with the stem-loop structures. Therefore, the type of the downstream secondary structure (stem-loop or pseudoknot) is not determined by the slippery sequence. The optimal frameshift efficiency required for the specific virus is guaranteed with the combination of the slippery sequence, spacer region 1 length and secondary structure element.

Acknowledgements

We wish to thank Dr. Kristiina Mäkinen for encouraging discussions, Dr. Aivar Liiv, Dr. Ülo Maiväli, Prof. Tanel Tenson and Prof. Jaanus Remme for expert help with chemical probing experiments and Signe Nõu for excellent plant care. This work was funded by Estonian Science Foundation grant no. 7363.

Appendix A. Supplementary data

Supplementary data associated with this article can be found, in the online version, at doi:10.1016/j.virusres.2009.09.002.

References

Abdelkafi, M., Ghomi, M., Turpin, P.Y., Baumruk, V., Hervé du Penhoat, C., Lampire, O., Bouchemal-Chibani, N., Goyer, P., Namane, A., Gouyette, C., Huynh-Dinh, T., Bednárová, L., 1997. Common structural features of UUCG and UACG tetraloops in very short hairpins determined by UV absorption, Raman, IR and NMR spectroscopies. J. Biomol. Struct. Dyn. 14, 579–593.

Baranov, P.V., Henderson, C.M., Anderson, C.B., Gesteland, R.F., Atkins, J.F., Howard, M.T., 2005. Programmed ribosomal frameshifting in decoding the SARS-CoV genome. Virology 332, 498–510.

Brierley, I., Dos Ramos, F.J., 2006. Programmed ribosomal frameshifting in HIV-1 and the SARS-CoV. Virus Res. 119, 29–42.

Brierley, I., Jenner, A.J., Inglis, S.C., 1992. Mutational analysis of the “slippery-sequence” component of a coronavirus ribosomal frameshifting signal. J. Mol. Biol. 227, 463–479.

Falk, H., Mador, N., Udi, R., Panet, A., Honigman, A., 1993. Two cis-acting signals control ribosomal frameshift between human T-cell leukemia virus type II gag and pro genes. J. Virol. 67, 6273–6277.

Giedroc, D.P., Cornish, P.V., 2008. Frameshifting RNA pseudoknots: structure and mechanism. Virus Res. 139, 193–208.

Giedroc, D.P., Theimer, C.A., Nixon, P.L., 2000. Structure, stability and function of RNA pseudoknots involved in stimulating ribosomal frameshifting. J. Mol. Biol. 298, 167–185.

Kim, K.H., Lommel, S.A., 1994. Identification and analysis of the site of -1 ribosomal frameshifting in red clover necrotic mosaic virus. Virology 200, 574–582.

Kim, K.H., Lommel, S.A., 1998. Sequence element required for efficient -1 ribosomal frameshifting in red clover necrotic mosaic dianthovirus. Virology 250, 50–59.

Kim, Y.G., Maas, S., Wang, S.C., Rich, A., 2000. Mutational study reveals that tertiary interactions are conserved in ribosomal frameshifting pseudoknots of two luteoviruses. RNA 6, 1157–1165.

Kim, Y.G., Su, L., Maas, S., O'Neill, A., Rich, A., 1999. Specific mutations in a viral RNA pseudoknot drastically change ribosomal frameshifting efficiency. Proc. Natl. Acad. Sci. U.S.A. 96, 14234–14239.

Kontos, H., Napthine, S., Brierley, I., 2001. Ribosomal pausing at a frameshifter RNA pseudoknot is sensitive to reading phase but shows little correlation with frameshift efficiency. Mol. Cell. Biol. 21, 8657–8670.

Liiv, A., Remme, J., 2004. Importance of transient structures during post-transcriptional refolding of the pre-23 S rRNA and ribosomal large subunit assembly. J. Mol. Biol. 342, 725–741.

Liiv, A., Tenson, T., Margus, T., Remme, J., 1998. Multiple functions of the transcribed spacers in ribosomal RNA operons. Biol. Chem. 379, 783–793.

Li, L., Wang, A.L., Wang, C.C., 2001. Structural analysis of the -1 ribosomal frameshift elements in giardiavirus mRNA. J. Virol. 75, 10612–10622.

Lucchesi, J., Mäkeläinen, K., Merits, A., Tamm, T., Mäkinen, K., 2000. Regulation of -1 ribosomal frameshifting directed by cocksfoot mottle sobemovirus genome. Eur. J. Biochem. 267, 3523–3529.

Maiväli, Ü., Pulk, A., Loogväli, E.L., Remme, J., 2002. Accessibility of phosphates in domain I of 23 S rRNA in the ribosomal 50S subunit as detected by R(P) phosphorothioates. Biochim. Biophys. Acta 1579, 1–7.

Marcheschi, R.J., Staple, D.W., Butcher, S.E., 2007. Programmed ribosomal frameshifting in SIV is induced by a highly structured RNA stem-loop. J. Mol. Biol. 373, 652–663.

Marczinke, B., Bloys, A.J., Brown, T.D., Willcocks, M.M., Carter, M.J., Brierley, I., 1994. The human astrovirus RNA-dependent RNA polymerase coding region is expressed by ribosomal frameshifting. J. Virol. 68, 5588–5595.

McGavin, W.J., Macfarlane, S.A., 2009. Rubus chlorotic mottle virus, a new sobemovirus infecting raspberry and bramble. Virus Res. 139, 10–13.

Meier, M., Paves, H., Olspert, A., Tamm, T., Truve, E., 2006. P1 protein of Cocksfoot mottle virus is indispensable for the systemic spread of the virus. Virus Genes 32, 321–326.
Meier, M., Truve, E., 2007. Sobemoviruses possess a common CfMV-like genomic organization. Arch. Virol. 152, 635–640.
Michiels, P.J., Versleijen, A.A., Verlaan, P.W., Pleij, C.W., Hilbers, C.W., Heus, H.A., 2001. Solution structure of the pseudoknot of SRV-1 RNA, involved in ribosomal frameshifting. J. Mol. Biol. 310, 1109–1123.
Molinaro, M., Tinoco Jr., I., 1995. Use of ultra stable UNCG tetraloop hairpins to fold RNA structures: thermodynamic and spectroscopic applications. Nucleic Acids Res. 23, 3056–3063.
Mäkinen, K., Naess, V., Tamm, T., Truve, E., Aaspõllu, A., Saarma, M., 1995a. The putative replicase of the cocksfoot mottle sobemovirus is translated as a part of the polyprotein by -1 ribosomal frameshift. Virology 207, 566–571.
Mäkinen, K., Tamm, T., Naess, V., Truve, E., Puurand, U., Munthe, T., Saarma, M., 1995b. Characterization of cocksfoot mottle sobemovirus genomic RNA and sequence comparison with related viruses. J. Gen. Virol. 76, 2817–2825.
Namy, O., Moran, S.J., Stuart, D.I., Gilbert, R.J., Brierley, I., 2006. A mechanical explanation of RNA pseudoknot function in programmed ribosomal frameshifting. Nature 441, 244–247.
Napthine, S., Liphardt, J., Bloys, A., Routledge, S., Brierley, I., 1999. The role of RNA pseudoknot stem 1 length in the promotion of efficient -1 ribosomal frameshifting. J. Mol. Biol. 288, 305–320.
Pallan, P.S., Marshall, W.S., Harp, J., Jewett III, F.C., Wawrzak, Z., Brown II, B.A., Rich, A., Egli, M., 2005. Crystal structure of a luteoviral RNA pseudoknot and model for a minimal ribosomal frameshifting motif. Biochemistry 44, 11315–11322.
Pennell, S., Manktelow, E., Flatt, A., Kelly, G., Smerdon, S.J., Brierley, I., 2008. The stimulatory RNA of the Visna-Maedi retrovirus ribosomal frameshifting signal is an unusual pseudoknot with an interstem element. RNA 14, 1366–1377.
Plant, E.P., Pérez-Alvarado, G.C., Jacobs, J.L., Mukhopadhyay, B., Hennig, M., Dinman, J.D., 2005. A three-stemmed mRNA pseudoknot in the SARS coronavirus frameshift signal. PLoS Biol. 3, e172.
Reeder, J., Steffen, P., Giegerich, R., 2007. pknotsRG: RNA pseudoknot folding including near-optimal structures and sliding windows. Nucleic Acids Res. 35 (Web Server issue), W320–W324.
Sérémé, D., Lacombe, S., Konaté, M., Pinel-Galzi, A., Traoré, V.S., Hébrard, E., Traoré, O., Brugidou, C., Fargette, D., Konaté, G., 2008. Biological and molecular characterization of a putative new sobemovirus infecting Imperata cylindrica and maize in Africa. Arch. Virol. 153, 1813–1820.
Shen, L.X., Tinoco Jr., I., 1995. The structure of an RNA pseudoknot that causes efficient frameshifting in mouse mammary tumor virus. J. Mol. Biol. 247, 963–978.
Staple, D.W., Butcher, S.E., 2005. Solution structure and thermodynamic investigation of the HIV-1 frameshift inducing element. J. Mol. Biol. 349, 1011–1023.
Stern, S., Moazed, D., Noller, H.F., 1988. Structural analysis of RNA using chemical and enzymatic probing monitored by primer extension. Methods Enzymol. 164, 481–489.
Su, L., Chen, L., Egli, M., Berger, J.M., Rich, A., 1999. Minor groove RNA triplex in the crystal structure of a ribosomal frameshifting viral pseudoknot. Nat. Struct. Biol. 6, 285–292.
Su, M.C., Chang, C.T., Chu, C.H., Tsai, C.H., Chang, K.Y., 2005. An atypical RNA pseudoknot stimulator and an upstream attenuation signal for -1 ribosomal frameshifting of SARS coronavirus. Nucleic Acids Res. 33, 4265–4275.
Tamm, T., Mäkinen, K., Truve, E., 1999. Identification of genes encoding for the cocksfoot mottle virus proteins. Arch. Virol. 144, 1557–1567.
Woese, C.R., Winker, S., Gutell, R.R., 1990. Architecture of ribosomal RNA: constraints on the sequence of "tetra-loops". Proc. Natl. Acad. Sci. U.S.A. 87, 8467–8471.
Yu, E.T., Zhang, Q., Fabris, D., 2005. Untying the FIV frameshifting pseudoknot structure by MS3D. J. Mol. Biol. 345, 69–80.